

# We are IntechOpen, the world's leading publisher of Open Access books Built by scientists, for scientists

5,800

Open access books available

142,000

International authors and editors

180M

Downloads

Our authors are among the

154

Countries delivered to

TOP 1%

most cited scientists

12.2%

Contributors from top 500 universities



WEB OF SCIENCE™

Selection of our books indexed in the Book Citation Index  
in Web of Science™ Core Collection (BKCI)

Interested in publishing with us?  
Contact [book.department@intechopen.com](mailto:book.department@intechopen.com)

Numbers displayed above are based on latest data collected.  
For more information visit [www.intechopen.com](http://www.intechopen.com)



# Advances in Resist Materials and Processing Technology: Photonic Devices Fabricated by Direct Lithography of Resist/Colloidal Nanocrystals Blend

Antonio Quattieri<sup>1</sup>, Tiziana Stomeo<sup>2</sup>, Luigi Martiradonna<sup>1</sup>,  
Roberto Cingolani<sup>1,2</sup> and Massimo De Vittorio<sup>1,2</sup>

*Italian Institute of Technology (IIT), Center for Bio-Molecular Nanotechnology  
National Nanotechnology Lab. of CNR/INFM, Scuola superiore ISUFI  
Italy*

## 1. Introduction

Lithographic techniques are the major driving force for the development of new photonic nanostructures. A wide range of techniques have been and are being developed for nano fabrication: e.g., deep UV ( $\lambda=200\text{--}290\text{ nm}$ ) and extreme UV ( $\lambda < 200\text{ nm}$ ) photolithography, electron-beam lithography (EBL), focused ion beam (FIB) lithography, X-ray lithography, scanning probe lithography, and others.

The degree of accuracy, reproducibility and resolution guaranteed by lithographic techniques is definitely better than other nanofabrication processes, such as wet and dry etching, sputtering, evaporation and so on. For this reason, "all-lithographic" fabrication protocols are being proposed for the realization of photonic devices based on non-conventional materials such as organic fluorophores or wet-chemical synthesized colloidal nanocrystals (NCs), whose exploitation in nano-optoelectronics is more recent as compared with epitaxially grown semiconductor emitters.

A potential approach for the fabrication of novel nanophotonic and nanoelectronic devices without recurring to traditional semiconductor processing technologies is represented by direct lithography of polymeric resists embedding active materials. For this purpose, colloidal nanocrystals appear as a promising active medium to be embedded into the hosting polymer, since they provide, with a high photochemical stability, emission wavelengths tunable from ultraviolet to infrared spectral region, high fluorescence efficiency, broad excitation spectra and narrow emission bands also at room temperature. Direct lithography of resist/NCs blends has proved to be an efficient strategy for the nanopositioning of NCs while preserving both the optical properties of the active material and the lithographic sensitivity of the hosting resist. The possibility of selectively localize semiconductor NCs on a substrate can lead to the fabrication of high performing photonic devices with novel active materials significantly cheaper than the traditional epitaxially grown active layers. The chapter is devoted to the presentation of several demonstrators of this innovative technique. Moreover, a survey of the fabrication results achieved by

Source: Lithography, Book edited by: Michael Wang,  
ISBN 978-953-307-064-3, pp. 656, February 2010, INTECH, Croatia, downloaded from SCIYO.COM

exploiting direct lithography of NCs/resist blends is reported, also discussing present limitations and future development of NC-based photonic devices.

## 2. Nanocrystals localization and device fabrication

As colloidal nanocrystals are dispersed in liquid solution, in order to be integrated in solid state devices they must be directly deposited on a substrate or embedded in a matrix. In the last years, some interesting results have been shown in literature about the deposition and the realization of nanocrystal-based devices.

Eisler et al. (2002) realized surface-emitting DFB laser structures by spin coating a NC/titania thin film on top of the grating previously realized by standard lithographic and dry etching processes. In this example, the matching between the Bragg condition of the grating and the ASE peak of the nanocrystal/titania film has been reached by modulating the grating periodicities and the volume fraction of nanocrystals by varying spinning speed. By using this strategy single wavelength DFB laser have been easily obtained, while multiple-wavelength lasers are harder to be constructed by simply spin-coating films on top of pre-formed gratings. In this sense, another strategy implemented by Sundar et al. (2004), consists in the typical “bottom-up” approach combining the processing ease afforded by semiconductor nanocrystals with soft lithography. The used scheme is described in Fig. 1. In particular, the NC films have been spin coated on a substrate and then embossed with a poly(dimethylsiloxane) (PDMS) elastomeric stamp. After thermal curing the successfulness of the technique has been verified by assessing the efficient diffraction of the light. Following a progressive assembly of multiple layers with well-matched gain at multiple wavelengths, these layers have been sequentially spin-coated and embossed. As a result, a multiple wavelength distributed feedback (DFB) laser oscillating simultaneously at room temperature has been obtained.

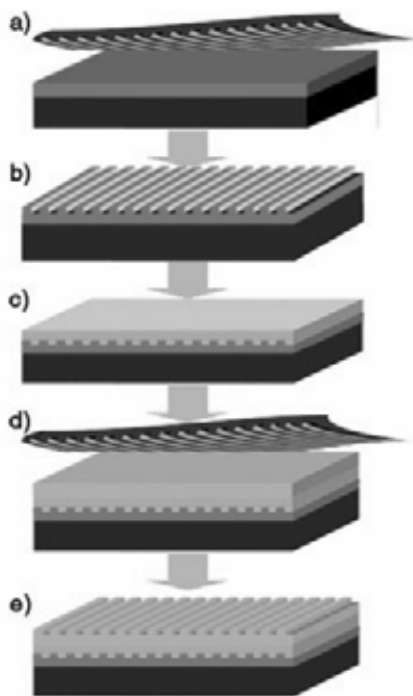


Fig. 1. Schematic illustration of the employed embossing strategy (Sundar et al., 2004).

A more efficient enhancement of the emission from colloidal nanocrystals has been obtained by Wu et al. (2007), by coupling NCs to an advanced photonic structure such as photonic crystal microcavities. In this device the deposition of PbSe quantum dots has been realized by dip-coating the patterned substrate in solutions of as-synthesized nanocrystals (Fig. 2). This strategy allows a significant enhancement of spontaneous emission strictly connected to the microcavity design but it is not able to control the positioning of the nanoemitters on the patterned substrate.

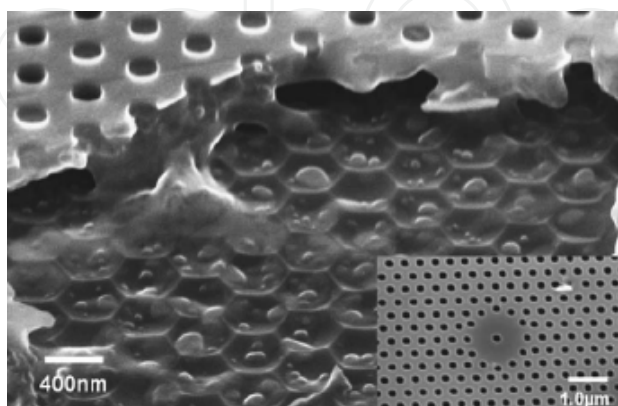


Fig. 2. Scanning electron microscope (SEM) image of a cleaved section of the two-dimensional photonic crystal microcavity showing PbSe quantum dots attached inside. The inset represents a SEM image in plane of the photonic crystal microcavity (Wu et al., 2007).

A better control on the micrometer scale has been achieved by Jun et al. (2006), with the exposure of a nanocrystals film to an UV source for the integration of nanocrystals in light-emitting devices. The direct lithography of nanocrystals films allowed the oleic acid ligands on the surface of the nanocrystals to form an insoluble cross-linked network while the unexposed areas were still soluble to toluene solvent (Fig. 3).

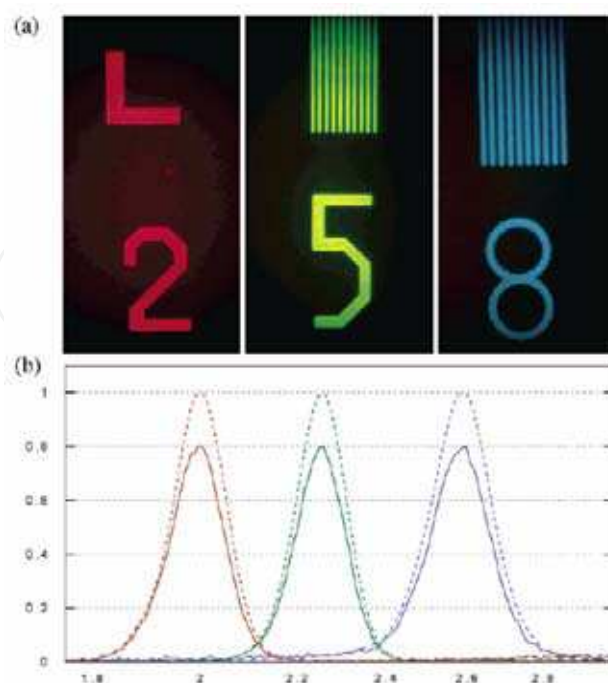


Fig. 3. (a) fluorescence micrograph and (b) PL spectra of the nanocrystal patterns (Jun et al., 2006)

Although, the UV light exposure through a shadow mask, could represent an appealing approach to the positioning of nanocrystals, it is limited due to the presence of a bottom layer and to the non guiding properties of the patterned structures.

These examples, even if not exhaustive, exploit the peculiar properties of the nanocrystals but all suffer from some deficiencies: i.e. they do not provide precise positioning and control on the lateral confinement of the waveguiding structure. Moreover, they require specific adherence properties as a function of the substrates and present low throughput.

The dispersion of these quantum dots into polymeric matrices proved to be a more powerful strategy: as it will be described in the next section, the chemical stability of semiconductor NCs together with their easy functionalization and the optical and electrical characteristics of organic materials lead to a new class of composite materials which better preserve the emission of quantum dots and show a good degree of processability (Fushman et al., 2005; Dick et al., 2004).

### 3. Nanocrystals-based devices fabricated by direct lithography

#### 3.1 Proof of the technique

To localize colloidal quantum dots by lithographic techniques, the affinity between the nanocrystals and the most common resists exploited in nanolithography has to be proved. Martiradonna et al. (2006a, 2006b) tested for their experiment Polymethylmethacrylate (PMMA) and SU-8. The first is a positive e-beam resist, while the second is a negative resist, both sensitive to e-beam and UV radiation respectively. Moreover, core/shell CdSe/ZnS nanocrystals have been prepared and diluted in chlorobenzene ( $C_6H_5Cl$ ) using standard methods (Reiss et al., 2002). The core/shell configuration has been preferred due to the higher chemical stability and quantum efficiency. The semiconductor clusters with different size have been dispersed with different molar concentration in PMMA-950K and SU-8 in order to understand the influence of the concentration and size of NCs on the lithographic properties of the blends. Then, a test pattern composed by a two-dimensional triangular lattice of pillars with sub-micron diameter has been defined in the PMMA layer by an e-beam lithography process. The contrast curve of the blend by testing several doses has been measured, in order to derive the sensitivity of the composite material to the beam. By means of an UV exposure, stripes ranging from 2  $\mu m$  to 100  $\mu m$  have been patterned on the SU-8 layer. In order to validate the technique, the optical properties of colloidal nanocrystals before and after the lithographic processes have been verified by collecting photoluminescence (PL) spectra at room temperature on the test samples through a confocal laser scanning microscope, with in-plane spatial resolution of 200 nm. A laser diode emitting at  $\lambda_{ex} = 405$  nm has been used as the excitation source.

As it can be observed by the two PL maps (shown in false colours in Fig. 4a and 4b), no emission has been detected from the regions of the blends which have been removed after development (black areas), thus confirming the removal of nanocrystals together with soluble resist. Moreover, by comparing the emission of the localized quantum dots (red and green lines in Fig. 4c) with the original photoluminescence spectrum (black line), no significant changes have been observed. This means that, thanks to the optical stability of these core/shell emitters, no relevant structural modifications or degradation of the optical properties are detected, also after the exposure to accelerated electrons or ultraviolet radiation.

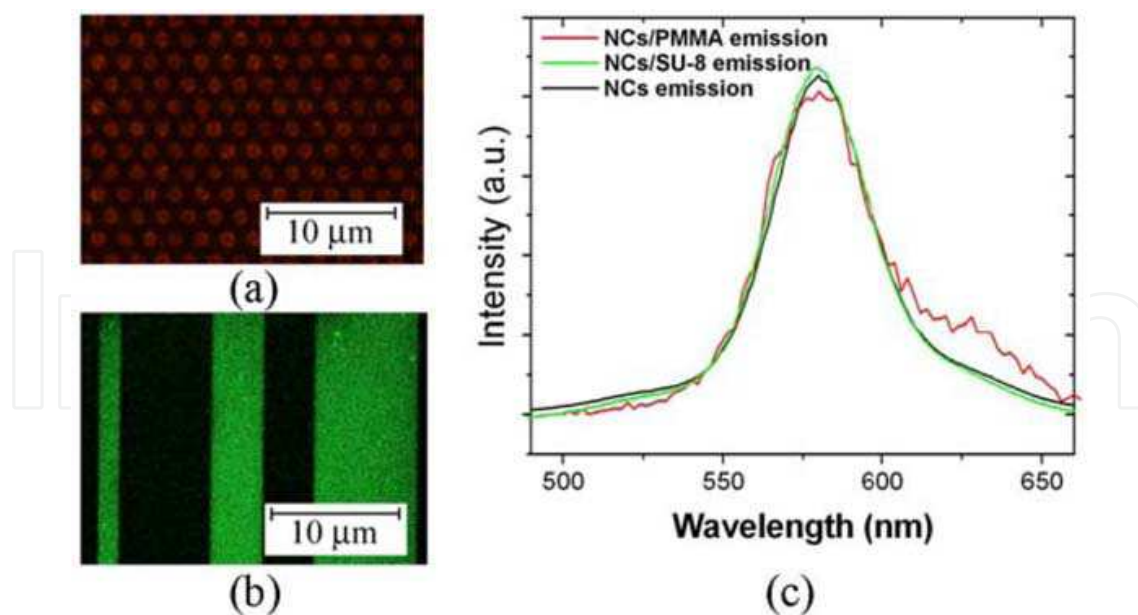


Fig. 4. (a) PL map (in false colours) of PMMA/NCs pillars after the e-beam lithographic process; (b) PL map (in false colours) of SU-8/NCs stripes after the photolithographic process; (c) Emission spectra detected on the patterned PMMA/NCs pillars (red line) and on the patterned SU-8/NCs stripes (green line), as compared to the emission of pure NCs in liquid solution (black line) (arranged from Martiradonna et al., 2006a, 2006b).

In the following subsections, this technique has been exploited to demonstrate the successful fabrication of the main building blocks of photonic systems such as: multicoloured devices, waveguide structures, suspended stripes and photonic crystal nanocavities.

### 3.2 Multicoloured devices

The fabrication of multicoloured micro- and nano- displays by realigned photolithographic steps or mix-and-match electron beam and photolithographic approaches has been recently demonstrated (Qualtieri et al., 2009a). Fully-customable micro- and nano- patterns can be obtained by a single lithographic procedure. Importantly, the possibility to re-align subsequent lithographic steps on the same substrate (as schematically shown in Fig. 4) enables the localization of different NCs ensembles in confining or superimposed regions. Thus, this technique has been exploited for the realization of RGB pixels on the micrometer scale, by localizing red, green and blue emitting nanocrystals in contiguous regions. The overall photoluminescence of each pixel results in the sum of the intensities of these chromatic components. By controlling the molar concentrations of the NCs and by varying the geometrical parameters of the localized patterns, the authors can finely tune the PL spectrum of these pixels thus obtaining multicoloured and white micro and nanoemitters.

In order to demonstrate the potential of this technique, the authors have reported the multicoloured logo of their affiliation by localizing two different ensembles of NCs. A first logo has been realized by exploiting two photolithographic steps: red-emitting nanocrystals dispersed in SU-8 ( $M_{\text{NCs}}=7.2 \cdot 10^{-6}$  mol/l), have been spin-coated on a Silicon substrate and exposed to ultraviolet radiation; after development and thermal curing, a second layer of green emitting NCs dispersed in SU-8 has been deposited on the sample and exposed. The sample has been finally developed and optically characterized by means of a confocal

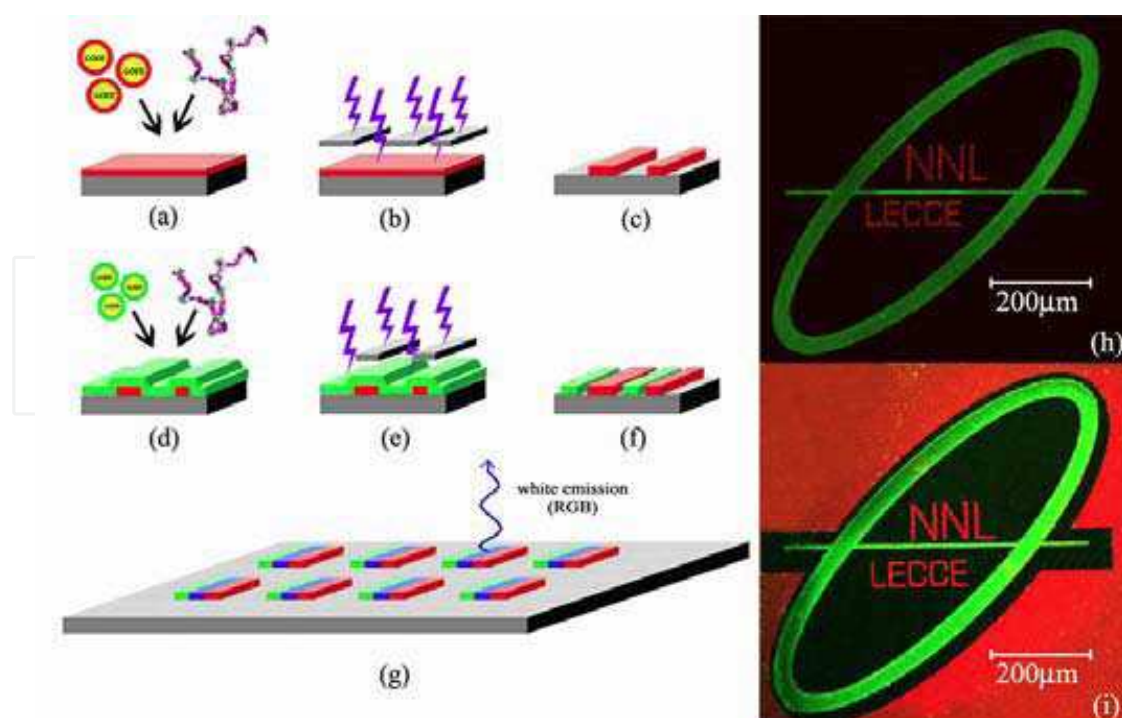


Fig. 4. Scheme of a realignment process for the localization of different ensembles of colloidal nanocrystals on the same substrate with lithographic techniques (Qualtieri et al. 2009a).

microscope. The combined fluorescence map, collected in two separate spectral ranges and shown in Fig. 4(h), demonstrates that no mixing between the two NCs ensembles can be detected, showing that the localization approach is not affected by the two sequential steps of the lithographic process.

Similarly, a second logo has been realized in mix-and-match lithography: a layer of PMMA containing red-emitting nanocrystals has been patterned through an e-beam lithography process, in order to selectively remove the red emitters from the exposed area. After development, a second layer of green/SU-8 blend has been spin-coated on the sample and patterned through photolithography. The photoluminescence map of the processed logo is reported in Fig. 4(i): the solvents used for PMMA and SU-8 polymers (chlorobenzene and cyclopentanone, respectively) has been verified being orthogonal (i.e. the already deposited layers are insoluble in the subsequent solvents), therefore well defined and distinguished colored regions are detected at the end of the process.

Furthermore, the authors also verified the possibility to combine the emission of different NCs ensembles by performing localization on superimposed regions. The CIE (Commission Internationale de l'Éclairage) coordinates of the emitted light have been calculated and has been found that the emission detected from superimposed patterns is a linear combination of red and green NCs emission. By increasing the green-to-red molar concentration ratio per unit area, the corresponding CIE coordinates shift from the red towards the green region, turning to a yellowish colour.

In this way, the possibility to realize multicoloured pattern by exploiting precise localization of colloidal nanocrystals dispersed in polymeric blends sensitive to electron beam or ultraviolet radiation has been demonstrated. This technology has been actually verified with red and green emitting quantum dots, but it can be also extended to blue emitters. In this

way, the full RGB colour range can be covered by exploiting just three NCs ensembles, and white emitting pixels can be easily obtained.

Moreover, the possibility to combine this technology with electrical injection already proposed for quantum dots based single-coloured LEDs (Sun et al., 2007), will allow the realization of bright, stable and cheap high resolution multicolour displays, for the next generation of video systems.

### 3.3 Waveguide photonic devices based on colloidal nanocrystal emitters

The top-down approach based on the dispersion of CdSe/ZnS core/shell NCs into a layer of electro-sensitive resist PMMA, has been exploited for the fabrication of distributed feedback (DFB) structures and distributed Bragg reflectors (DBR) suitable for the realization of in-plane waveguide lasers (Martiradonna et al., 2007).

To this aim, nanocrystals emitting at 640 nm have been dispersed in PMMA-950K positive resist with a molar concentration of  $M_{\text{NCs}} = 2.51 \times 10^{-5}$  mol/l. This high loading fraction of the nanoemitters increases the refractive index value of PMMA from 1.49 to 1.62 at  $\lambda = 640$  nm, thus allowing the index confinement of visible light into PMMA/NCs waveguides fabricated on glass substrates.

Two realigned lithographic steps have been used and a single development of the resist has been carried out after both the lithographic steps with different beam parameters, without recurring to following etching processes. In particular, the optimized electron beam lithography (EBL) parameters have been used on a PMMA/NCs film in order to pattern a 100  $\mu\text{m}$  long, 30  $\mu\text{m}$  wide active ridge cavity and two distributed Bragg reflectors composed by alternating  $3\lambda/4$  thick stripes of PMMA/NCs and air. A 20 pairs back DBR and a 10 pairs front DBR have been obtained by exposing 480 nm wide stripes having a period of 780 nm.

The second e-beam lithographic process has been used to define, by a shallow removal of the blend, a DFB on the waveguide by creating a periodical corrugation on the top of the waveguide. A single development step of the resist has been carried out after both the two lithographic steps with different beam parameters.

The active blend has been removed from the sides of the ridge cavity (dark lateral regions) and from the stripes of the DBR (as shown in Fig. 5).

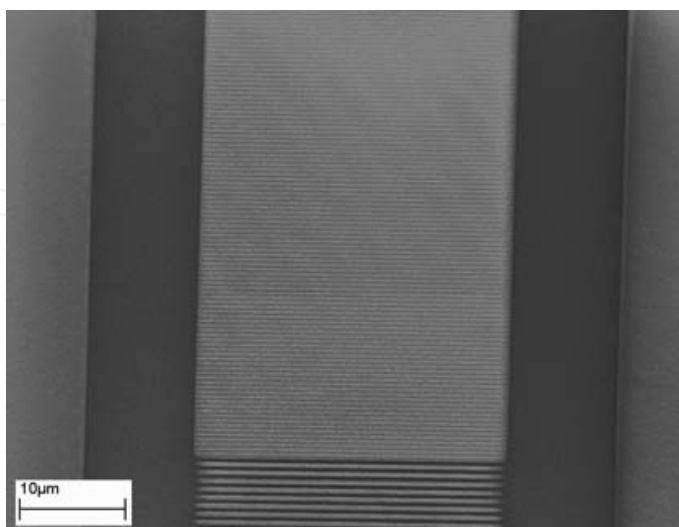


Fig. 5. SEM image of the ridge cavity obtained by localizing the PMMA/NCs by means of EBL processes (arranged from Martiradonna et al 2007).

The main advantage of this all-lithographic localization approach is the extreme versatility, which allows the implementation of mostly any geometry required by the laser designer, with resolutions pushed down to the nanometre scale. Moreover, also the optical properties (optical gain, emission wavelength, refractive index) of the active material can be arbitrarily tuned by simply varying the size and the density of the emitters dispersed in the resist. The possibility to re-align multiple lithographic steps on the same substrate allows also the localization of different active blends on near or even superimposed regions, thus realizing multi-wavelength laser sources on a single device. Importantly, since this technique can be applied to any kind of substrate, also the fabrication of DFB lasers on flexible surfaces can be enabled. As a straightforward application, optical sensors detecting strain-induced variations of the DFB corrugation period, and therefore of the lasing wavelength, could be obtained.

### 3.4 Colloidal nanocrystals air bridge fabricated by direct lithography

Membrane structures, also called air bridges, are suspended structures completely surrounded by air. Since the bridge is completely surrounded by low index claddings (either air or low-index materials) a strong light confinement and efficient waveguiding can be obtained. Passive suspended waveguides and Photonic Crystals based suspended filters (Carlsson et al., 2002), able to model the transmitted light, have been fabricated. Nanolasers coupling 2D PhC microcavities on semiconductor bridges with active InGaAsP quantum wells (Loncar et al. 2004) are also being developed both as infrared light sources and for optical sensors. In this sense, Quattieri et al., (2007) demonstrated that the lithography based localization approach proved to be effective in the fabrication of 3D geometries like NCs air bridges by cyclically depositing and exposing different blends of nanoemitters/resists on the same substrate, with no recursion to following etching steps.

To this aim, two different ensembles of core/shell CdSe/ZnS nanocrystals, emitting in the red and green region, have been prepared and dispersed in a SU-8 negative photoresist matrix. Stripes with varying spacing from 6  $\mu\text{m}$  up to 120  $\mu\text{m}$  have been localized by exposing the red active film to the ultraviolet radiation of a KARL-SUSS MJB3 mask aligner (Hg i-line at  $\lambda = 365 \text{ nm}$ ) with an exposure dose of 0.87 J. A post exposure bake (PEB) has been performed on the prototype, but it has not been developed in order to preserve its surface planarity. On this sample a second 1500 nm thick layer of green-emitting NCs has been spin-coated and thermal cured. A second array of perpendicular stripes with varying widths (2  $\mu\text{m}$  - 20  $\mu\text{m}$ ) has been localized by means of an UV exposure (exposure dose = 0.87 J). After the PEB, the sample has been developed into SU-8 developer for 1 min. SEM measurements performed on the fabricated prototype tilted at 45° assessed the obtained 3D structures (Fig. 6a).

Moreover, photoluminescence images collected by means of a confocal laser microscope reveal the green and red emitting regions on the sample (Fig. 6(b)). Red PL collected in the 630–670 nm spectral range shows a bright emission only from the first layer, while green PL (collected in the 530–570 nm spectral range) is detected only from the suspended bridges.

Fig. 6(c) compares the emission spectra coming from a stripe of the first layer (circle line), from a stripe of the second layer (triangle line) and from an unpatterned zone (solid line). As it is evident from the latter spectrum, the localization of both the ensembles of NCs is perfectly controlled with this lithographic approach since in unexposed regions of both layers no PL signal is detected. Thanks to the optical transparency of SU-8 at in the whole

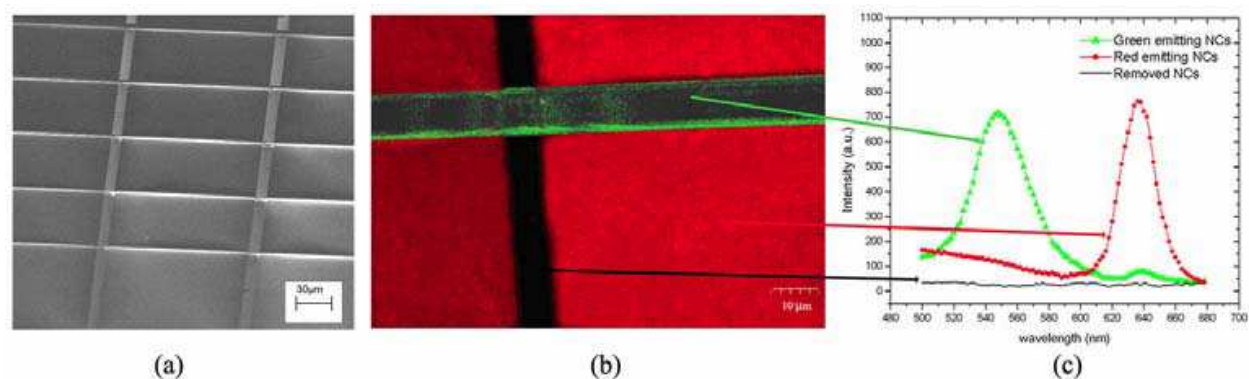


Fig. 6. a) SEM image of the fabricated air bridge structure; b) Superposition of two (PL) maps of the fabricated sample, collected in the 530 – 570 nm spectral range (green) and in the 630 – 670 nm spectral range (red); c) emission spectra coming from the regions in which only red NCs are localized (circle line), only green NCs are localized (triangle line) and both the blends are removed (square line) (arranged from Quattieri et al., 2007).

visible spectral range, the red emission coming from the underlying layer is detected also through the green emitting layer (triangle line). The PL increase, shown in the blue range (400 – 500 nm) both in circle and triangle lines, is due to a slight emission coming from the polymeric matrix after its exposure to UV light.

Active 3D photonic crystals and woodpile structures can be implemented in the whole visible spectral range, but also in the ultraviolet and infrared range by properly tuning the optical properties of the NCs dispersed in the blend.

### 3.5 Active photonic crystal structures fabricated on suspended membranes

The insertion of nanoemitters into photonic crystal (PhC) cavities with localized optical modes having high quality factor (Q) and small modal volume has been exploited to tailor both the spatial and spectral properties of the NCs radiation. In fact, colloidal nanocrystals confined into two-dimensional PhCs are promising candidates for the development of next generation high performing optical devices such as single photon sources, ultralow threshold lasers, and nonlinear devices. At present, several works have been proposed in order to couple colloidal NCs to 2D-PC structures fabricated on Si or AlGaAs membrane layers (Wu et al., 2007; Fushman et al., 2005). In these reported cases, high Q passive nanocavities have been previously fabricated on solid substrates then PbS or PbSe colloidal nanocrystals emitting in the infrared spectral range have been added by dipping or spin-coating techniques on top of the patterned layer. The coupling between the emitters and the quantum-confined optical environment has been demonstrated by the presence of resonant peaks in the photoluminescence spectra collected on the fabricated devices. This kind of approach requires a pattern transfer on the rigid membrane layer by high-resolution lithographic techniques and etching steps, which could introduce fabrication imperfections in the structure i.e. deviation of the hole radii, slightly angled sidewalls, high surface roughness after resist stripping. Moreover, these techniques can be only applied to infrared-emitting colloidal nanocrystals, due to high absorption of Si and AlGaAs in the visible spectral range. Direct lithography of NCs/blends allows the fabrication of semiconductor nanocrystal-based 2D-PhC nanocavities, without requiring pattern transfer from the resist to the underlying membrane layers, since the resist itself acts as the suspended waveguiding layer. The optical quality of the resonating structure is only determined by a single high-

resolution lithographic step, being not affected by any etching process. Moreover, the absence of absorbing layers from the visible to the infrared region of the spectrum allows the use of NCs on a large spectral range, thus conferring a broader applicability to this technique. Nevertheless, in this approach, a new type of semiconductor nanoemitters, which are dot-in-a-rod colloidal nanocrystals (DR-NCs) consisting of CdS rods nucleated at high temperatures around CdSe spherical seeds has been exploited (Carbone et al., 2007; Talapin et al., 2007). These elongated core-shell nanocrystals show remarkably high quantum efficiency (up to 70-75%), due to a high quantum yield coupled with a large extinction coefficient in the ultraviolet spectral range, the latter due to the presence of a thick CdS shell. By virtue of their high efficiency and photostability DR-NCs PL emission is easily detectable even at room temperature with no need of highly sensitive detection setup. Due to the low index contrast between the membrane and the surrounding air cladding, in order to increase the mode confinement, an approach similar to the graded square lattice proposed by Srinivasan & Painter (2002) has been followed by Martiradonna et al., (2008). For the practical realization of the device, a 1  $\mu\text{m}$  thick layer of  $\text{Al}_{0.7}\text{Ga}_{0.3}\text{As}$  has been epitaxially grown by metal-organic chemical vapor deposition (MOCVD) on GaAs substrate and a 320 nm thick layer of ZEP/NCs has been spin coated on top of it. Fig 7a shows an in-plane SEM image of the patterned structure after development. In order to remove the underlying sacrificial layer, the sample has been then dipped in a  $\text{HF}:\text{H}_2\text{O}$  etching solution at room temperature. It has been then rinsed with isopropyl alcohol with the aim to decrease the surface tension of the solvent during its evaporation in air. A sketch of the final structure after wet-etching is shown in Fig. 7b.

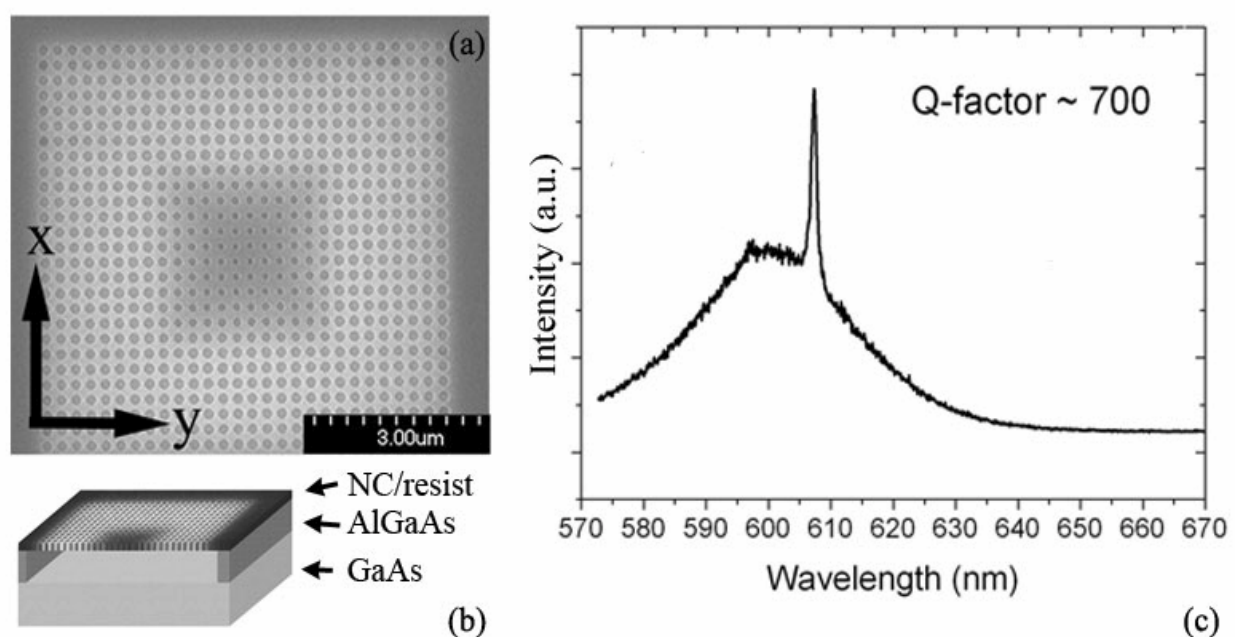


Fig. 7. a) and b) Scanning electron microscope image of the patterned nanocavity and sketch of the final membrane structure, (c) Output spectra of the nanocavity embedding nanoemitters (arranged from Martiradonna et al., 2008)

In order to verify the effectiveness of the fabrication process, micro-photoluminescence measurements at room temperature have been performed on the nanocavities and a Q-factor of 700 has been found (Fig. 7c). This new strategy for the fabrication of high-

performing NCs-based devices is very promising for the development of all-optical circuits that can be fully integrated with traditional Silicon technology.

### 3.6 Single colloidal nanocrystals in microcavity

Secure Quantum Communication Systems (QCS) based on the transmission of crucial information through single photons are among the most appealing frontiers for telecommunications, though their development is still hindered by the lack of cheap and bright Single Photon Sources (SPS) operating at room temperature. In this section we describe a high resolution direct lithographic technique for obtaining photon antibunching behavior at room temperature from single colloidal CdSe/ZnS nanocrystals (NCs) localized in a 1D-PhC microcavity (Quattieri et al. 2009b).

In order to verify the possibility to localize single nanocrystals by means of electron beam lithography, a dielectric structure, consisting of a SiO<sub>2</sub>/TiO<sub>2</sub>-based distributed Bragg reflector (DBR) and an additional SiO<sub>2</sub> spacing layer, has been preliminary fabricated. A very low concentration of CdSe/ZnS colloidal nanocrystals emitting at  $\lambda = 610$  nm has been dispersed in a high-resolution electron-beam resist, namely Hydrogen Silsesquioxane (HSQ) (Namatsu et al., 1998). A 90 nm thick layer of the blend has been spin-coated on the dielectric structure and subsequently exposed to the electron beam to define an array of active pillars with diameters ranging from 500 nm down to 30 nm. The emission spectrum of the array of nanopillars has been collected by means of a confocal microscope at room temperature. Remarkably, the array of nanoemitters showed different optical properties depending on the different dimensions of the pillars. Structures having a diameter above 100 nm showed a fluorescence typical of an ensemble of nanocrystals with a FWHM of about 30nm (Fig.8a, black line), whilst a narrower emission (FWHM  $\sim 19$  nm) has been collected from the smallest ones (Fig. 8a, blue line). The lorentzian shape of the latter PL spectrum, together with the typical blinking emission in time (Neuhauser et al., 2000), indicate the single photon nature of the source. The clear fingerprint of single photon emission, represented by the reduced probability of two photons being detected within a short time interval and namely the photon antibunching behaviour (Messin et al., 2001) of the luminescence, has been observed by analyzing the auto-correlation function of the emitted signal collected by means of a standard Hanbury-Brown and Twiss setup (Fig.8b).

Having successfully accomplished the control of the localization of single quantum emitters by the high resolution electron beam lithography (EBL) based approach, a complete planar microcavity as sketched in Fig. 9a (the detail of the cavity region is shown in Fig. 9b), cladding the array of pillars between two SiO<sub>2</sub>/TiO<sub>2</sub> DBRs has been realized. The microcavity has been designed to resonate at a wavelength of 610 nm.

Micro-photoluminescence analyses has been performed and the Fig. 10a shows a representative PL spectrum detected from a 90 nm-wide pillar. Its line-width is further reduced down to 12.3 nm with respect to the NCs ensemble luminescence in the cavity, since the presence of a single semiconductor emitter in the pillar causes lower absorption and scattering losses. The evidence of single photon generation is given, also in this case, by the measurement of the autocorrelation function of the emitted light, which reveals an antibunching behaviour at zero delay (see Fig. 10b).

The area of the peak at zero delay is equal to 0.27. After subtracting the signal corresponding to the background, this area is even lower with a value of 0.21. The normalized area of the peaks at nonzero delays goes up to 1.35, reflecting an additional bunching of the

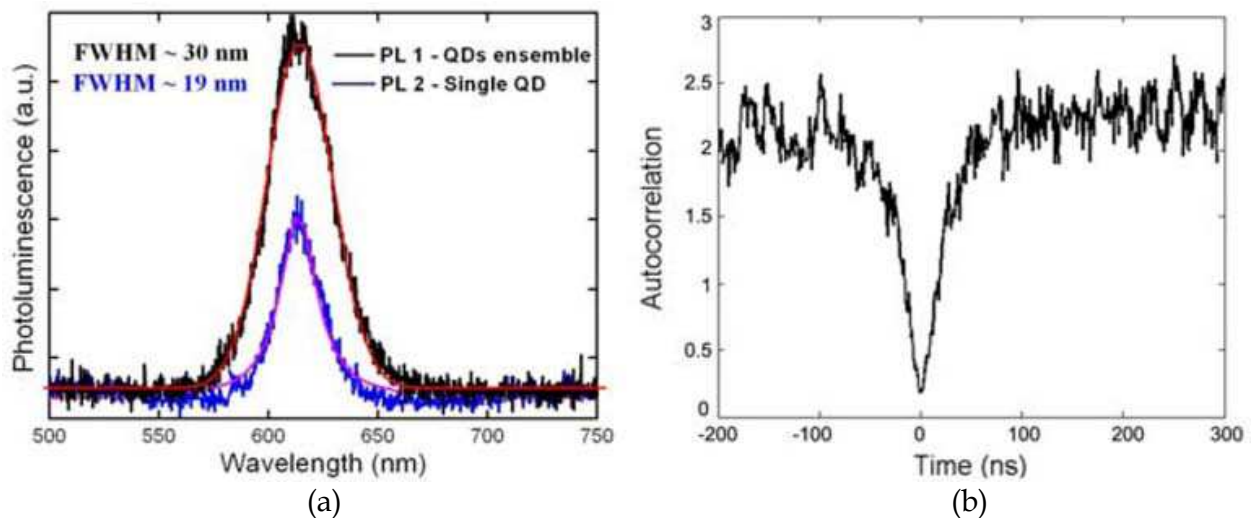


Fig. 8. (a) photoluminescence spectra showing the different line-shape depending on the different dimensions of the pillars (black line collected from a 500 nm wide pillar and blue line collected from a 90 nm wide pillar); (b) auto-correlation trace of the PL arising from a 90 nm wide pillar (normalized with background correction), showing an antibunching behaviour (arranged from Qualtieri et al., 2009b).

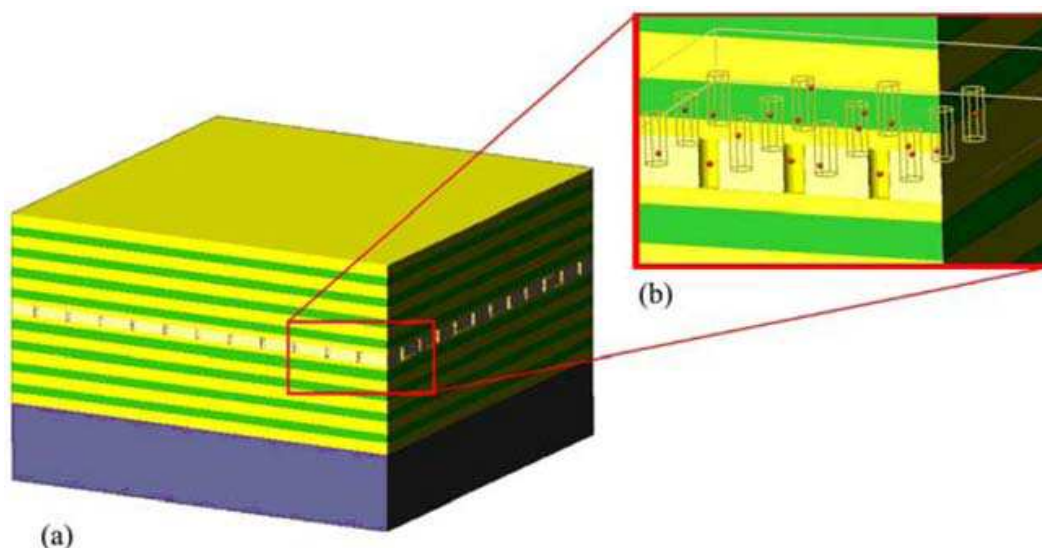


Fig. 9. (a) and (b): 3D- sketches of the whole structure and of the cavity region, respectively (arranged from Qualtieri et al., 2009b).

fluorescence due to the emission intermittency, as explained by Messin et al., (2001). Using the histogram of the coincidences counts, the lifetime of the excited state has been also deduced. The exponential fit of the experimental data collected from several SPSs gives an average radiative lifetime of  $\tau_{\text{cav}} \sim 9.1$  ns that compared to the decay lifetime of an ensemble of nanocrystals surrounded by HSQ not inserted in a cavity ( $\tau_{\text{fs}} \sim 23$  ns) showed a shortening of the radiative lifetime due to the wavelength-sized cavity.

The unprecedented photon antibunching behaviour observed from colloidal nanocrystals embedded in a planar microcavity, together with an efficient tailoring of the recombination decay rate at room temperature, confirms the suitability of this approach for the fabrication of SPSs based on colloidal nanocrystals, thus overcoming the limitation in the operating temperature shown by epitaxial quantum dot sources.

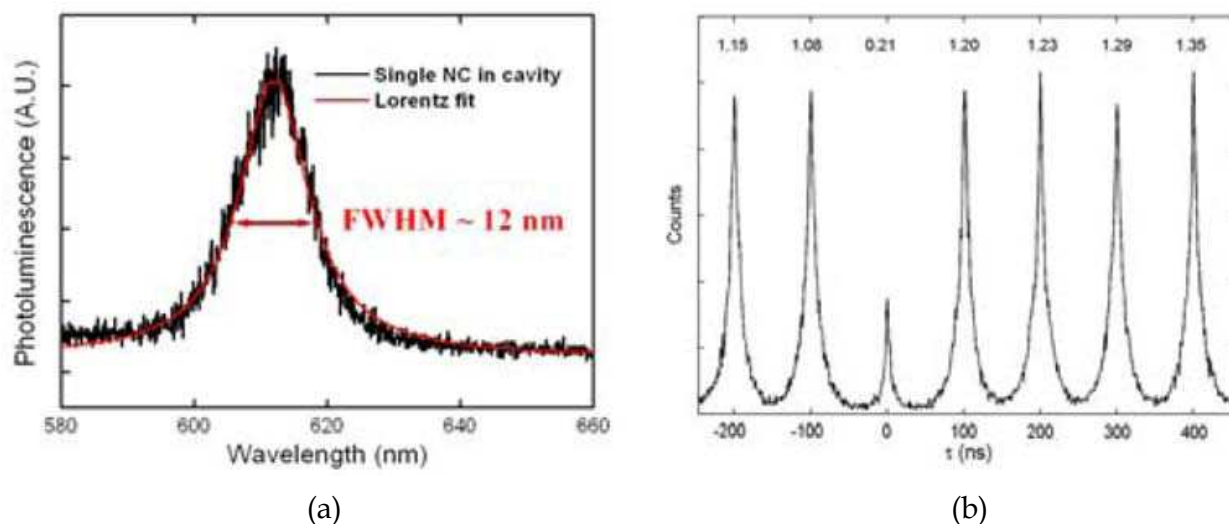


Fig. 10. (a) Room-temperature photoluminescence of a 90-nm wide pillar. (b) Histogram of coincidence counts of a single QD fluorescence. Above each peak the area normalized to Poissonian photon statistics, with background correction, is given (arranged from Qualtieri et al., 2009b).

#### 4. Conclusion

In this chapter, a novel approach for the direct lithographic fabrication of photonic devices based on colloidal quantum dots has been proposed. Different examples of nanocrystals localization and devices fabrication have been reported in section 2. They exploit the unique optical and spectroscopic properties of colloidal nanocrystals, but all of them suffer from some deficiency: they do not provide precise positioning and control on the lateral confinement of the waveguiding structure. Moreover, they require specific adherence properties in function of the substrates and present low throughput. On the contrary, the precise localization of colloidal NCs through the nanopatterning of active blends, without recurring to any preparation of the substrate, leads to broader applications in the nanophotonic field.

Successful examples of the fabrication approach able to manipulate blends composed of polymeric matrices and colloidal nanocrystals by exploiting peculiar characteristics of the hosting material have been reported:

- multicolour emitting devices obtained by the localization in nearby regions of different PMMA/QDs and SU8/QDs blends, in re-aligned e-beam and photo-lithography steps;
- PMMA/QDs blend-based in-plane waveguide devices with distributed Bragg reflectors and distributed feed-back patterns, fabricated by the subsequent exposures of the sample to e-beam lithography processes with different acceleration voltages;
- suspended air-bridge structures suitable for the fabrication of highly optical confined active waveguides. The release of the suspended structure has been performed in the development of the exposed sample, with no need of following chemical etching steps.

Moreover, it allowed to fabricate advanced photonic devices based on colloidal nanocrystal for integrated all-optical systems and information processing.

In particular, by exploiting both Photonic Crystals and NCs properties two different devices have been realized:

- 2D-PhC resist nanocavity, with a Q-factor of  $\sim 700$ , aiming to the realization of high-efficiency ultra-small lasers and non-classical light sources in the visible range;
- Single photon source (SPS) device based on 1D-PhC embedding colloidal nanocrystals with an enhancement of the radiative decay of  $\sim 2.4$  (as expected by theoretical prediction). The precise nanopatterning has been essential to define, by electron beam lithography, the nanometre feature size of the NCs/HSQ blend for SPS. This single photon device demonstrated for the first time antibunching behaviour of a single NC in microcavity at room temperature.

The presence of a controlled concentration of NCs in the resists does not modify their peculiar behaviour thus enabling the fabrication of 1D-2D and 3D active photonic crystals devices without recurring to etching processes.

As a consequence, the dispersion of wet chemically synthesized quantum dot in hosting materials sensitive to photo or electron beam radiation reveals to be a very promising and appealing strategy for the fabrication of innovative photonic devices, fully integrated with traditional Silicon technology.

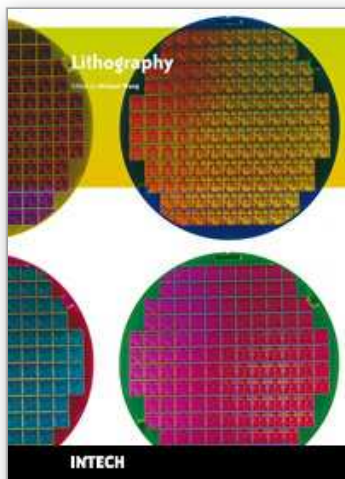
## 5. References

- Carbone, L.; Nobile, C.; De Giorgi, M.; Della Sala, F.; Morello, G.; Pompa, P. P.; Hytch, M.; Snoeck, E.; Fiore, A.; Franchini, I. R.; Nadasan, M.; Silvestre, A. F.; Chiodo, L.; Kudera, S.; Cingolani, R.; Krahn, R. & Manna, L. (2007). Synthesis and Micrometer-Scale Assembly of Colloidal CdSe/CdS Nanorods Prepared by a Seeded Growth Approach. *Nano Letters*, Vol. 7, No. 10 (September 2007) 2942-2950, ISSN 1530-6992
- Carlsson, N.; Ikeda, N.; Sugimoto, Y.; Asakawa, K.; Takemori, T.; Katayama, Y.; Kawai, N. & Inoue, K. (2002). Design, nano-fabrication and analysis of near-infrared 2D photonic crystal air-bridge structures. *Optical and Quantum Electronics*, Vol. 34 (January 2002) 123-131, ISSN 1572-817X
- Dick, K. A.; Deppert, K.; Larsson, M. W.; Martensson, T.; Seifert, W.; Wallenberg, L. R. & Samuelson, L. (2004). Synthesis of branched "nanotrees" by controlled seeding of multiple branching events. *Nature Materials*, Vol. 3 (May 2004) 380-384, ISSN 1476-1122
- Eisler, H. J.; Sundar, V. C.; Bawendi, M. G.; Walsh, M.; Smith, H. I. & Klimov, V. (2002). Color-selective semiconductor nanocrystal laser. *Applied Physics Letters*, Vol. 80 (June 2002) 4614-4616, ISSN 1077-3118
- Fushman, I.; Englund, D. & Vuckovic, J. (2005). Coupling of PbS quantum dots to photonic crystal cavities at room temperature. *Applied Physics Letters*, Vol. 87 (December 2005) 241102-1 - 241102-3, ISSN 1077-3118
- Jun, S.; Jang, E.; Park, J. & Kim, J. (2006). Photopatterned Semiconductor Nanocrystals and Their Electroluminescence from Hybrid Light-Emitting Devices. *Langmuir*, Vol. 22, No. 6 (February 2006) 2407-2410, ISSN 1520-5827
- Loncar, M.; Yoshie, T.; Okamoto, K.; Qiu, Y.; Vuckovic, J. & Scherer, A. (2004). Planar Photonic Crystal Nanolasers (I): Porous Cavity Lasers. *IEICE Transaction on Electronics*. Vol. E87-C, No. 3 (March 2004) 291-299, ISSN 0916-8516
- Martiradonna, L.; Stomeo, T.; De Giorgi, M.; Cingolani, R. & De Vittorio, M. (2006a). Nanopatterning of colloidal nanocrystals emitters dispersed in a PMMA matrix by

- e-beam lithography. *Microelectronic Engineering*, Vol. 83 (February 2006) 1478-1481, ISSN 0167-9317
- Martiradonna, L.; Stomeo, T.; Carbone, L.; Morello, G.; Salhi, A.; De Giorgi, M.; Cingolani, R. & De Vittorio, M. (2006b). Nanopositioning of colloidal nanocrystal emitters by means of photolithography and e-beam lithography. *Physica Status Solidi (b)*, Vol. 243 No. 15 (December 2006) 3972-3975, ISSN 1521-3951
- Martiradonna, L.; Qualtieri, A.; Stomeo, T.; Carbone, L.; Cingolani, R. & De Vittorio, M. (2007). Lithographic nano-patterning of colloidal nanocrystal emitters for the fabrication of waveguide photonic devices. *Sensors and Actuators B: Chemical*, Vol. 126, No. 1 (September 2007) 116-119, ISSN 0925-4005
- Martiradonna, L.; Carbone, L.; Tандаechanurat, A.; Kitamura, M.; Iwamoto, S.; Manna, L.; De Vittorio, M.; Cingolani, R. & Arakawa, Y. (2008). Two-Dimensional Photonic Crystal Resist Membrane Nanocavity Embedding Colloidal Dot-in-a-Rod Nanocrystals. *Nanoletters*, Vol. 8, No. 1, (December 2007) 260-264, ISSN 1530-6992
- Messin, G.; Hermier, J. P.; Giacobino, E.; Desbiolles, P. & Dahan, M. (2001). Bunching and antibunching in the fluorescence of semiconductor nanocrystals. *Optics Letters*, Vol. 26, No. 23 (December 2001) 1891-1893, ISSN 1539-4794
- Namatsu, H.; Yamaguchi, T.; Nagase, M.; Yamazaki, K. & Kurihara, K. (1998). Nano-patterning of a hydrogen silsesquioxane resist with reduced linewidth fluctuations. *Microelectronic Engineering*, Vol. 41 (March 1998) 331-334, ISSN 0167-9317
- Neuhauser, R. G.; Shimizu, K.T.; Woo, W. K.; Empedocles, S. A. & Bawendi, M. G. (2000) Correlation between Fluorescence Intermittency and Spectral Diffusion in Single Semiconductor Quantum Dots. *Physical Review Letters*, Vol. 85, No. 15 (October 2000) 3301-3304, ISSN 1079-7114
- Qualtieri, A.; Martiradonna, L.; Cingolani, R. & De Vittorio, M. (2007). Colloidal nanocrystals air bridge fabricated by direct lithography. *Microelectronic Engineering*, Vol. 84 (February 2007) 1488-1490, ISSN 0167-9317
- Qualtieri, A.; Martiradonna, L.; Stomeo, T.; Todaro, M. T.; Cingolani, R. & De Vittorio, M. (2009a). Multicolored devices fabricated by direct lithography of colloidal nanocrystals. *Microelectronic Engineering*, Vol. 86 (April 2009) 1127-1130, ISSN 0167-9317
- Qualtieri, A.; Morello, G.; Spinicelli, P.; Todaro, M. T.; Stomeo, T.; Martiradonna, L.; De Giorgi, M.; Quélin, X.; Buil, S.; Bramati, A.; Hermier, J. P.; Cingolani, R. & De Vittorio, M. (2009b). Nonclassical emission from single colloidal nanocrystals in a microcavity: a route towards room temperature single photon sources. *New Journal of Physics*, Vol. 11, No. 3 (March 2009) 033025-033034, ISSN 1367-2630
- Reiss, P.; Bleuse, J. & Pron, A. (2002). Highly Luminescent CdSe/ZnSe Core/Shell Nanocrystals of Low Size Dispersion. *Nanoletters*, Vol. 2 No. 7 (June 2002) 781-784, ISSN 1530-6992
- Srinivasan, K. & Painter, O. (2002). Momentum space design of high-Q photonic crystal optical cavities. *Optic Express*, Vol. 10, No. 15 (July 2002) 670-684, ISSN 1094-4087
- Sun, Q.; Wang, Y. A.; Li, L. S.; Wang, D.; Zhu, T.; Xu, J.; Tang, C. & Li, Y. (2007). Bright, multicoloured light-emitting diodes based on quantum dots. *Nature Photonics*, Vol. 1, No. 12 (November 2007) 717-722, ISSN 1749-4885
- Sundar, V. C.; Eisler, H. J.; Deng, T.; Chan, Y.; Thomas, E. L. & Bawendi, M. G. (2004). Soft-Lithographically Embossed, Multilayered Distributed-Feedback Nanocrystal

- Lasers. *Advanced Materials*, Vol. 16, No. 80, (December 2004) 2137-2141, ISSN 1521-4095
- Talpin, D. V.; Nelson, J. H.; Shevchenko, E. V.; Aloni, S.; Sadtler, B. & Alivisatos, A. P. (2007). Seeded Growth of Highly Luminescent CdSe/CdS Nanoheterostructures with Rod and Tetrapod Morphologies. *Nano Letters*, Vol. 7, No. 10 (September 2007) 2951-2959, ISSN 1530-6992
- Wu, Z.; Mi, Z.; Bhattacharya, P.; Zhu T. & Xu, J. (2007). Enhanced spontaneous emission at 1.55  $\mu\text{m}$  from colloidal PbSe quantum dots in a Si photonic crystal microcavity. *Applied Physics Letters*, Vol. 90 (April 2007) 171105-1 - 171105-3, ISSN 1077-3118

IntechOpen



## **Lithography**

Edited by Michael Wang

ISBN 978-953-307-064-3

Hard cover, 656 pages

**Publisher** InTech

**Published online** 01, February, 2010

**Published in print edition** February, 2010

Lithography, the fundamental fabrication process of semiconductor devices, plays a critical role in micro- and nano-fabrications and the revolution in high density integrated circuits. This book is the result of inspirations and contributions from many researchers worldwide. Although the inclusion of the book chapters may not be a complete representation of all lithographic arts, it does represent a good collection of contributions in this field. We hope readers will enjoy reading the book as much as we have enjoyed bringing it together. We would like to thank all contributors and authors of this book.

### **How to reference**

In order to correctly reference this scholarly work, feel free to copy and paste the following:

Antonio Qualtieri, Tiziana Stomeo, Luigi Martiradonna, Roberto Cingolani and Massimo De Vittorio (2010). Advances in Resist Materials and Processing Technology: Photonic Devices Fabricated by Direct Lithography of Resist/Colloidal Nanocrystals Blend, Lithography, Michael Wang (Ed.), ISBN: 978-953-307-064-3, InTech, Available from: <http://www.intechopen.com/books/lithography/advances-in-resist-materials-and-processing-technology-photonic-devices-fabricated-by-direct-lithogr>

# **INTECH**

open science | open minds

### **InTech Europe**

University Campus STeP Ri  
Slavka Krautzeka 83/A  
51000 Rijeka, Croatia  
Phone: +385 (51) 770 447  
Fax: +385 (51) 686 166  
[www.intechopen.com](http://www.intechopen.com)

### **InTech China**

Unit 405, Office Block, Hotel Equatorial Shanghai  
No.65, Yan An Road (West), Shanghai, 200040, China  
中国上海市延安西路65号上海国际贵都大饭店办公楼405单元  
Phone: +86-21-62489820  
Fax: +86-21-62489821

© 2010 The Author(s). Licensee IntechOpen. This chapter is distributed under the terms of the [Creative Commons Attribution-NonCommercial-ShareAlike-3.0 License](#), which permits use, distribution and reproduction for non-commercial purposes, provided the original is properly cited and derivative works building on this content are distributed under the same license.

IntechOpen

IntechOpen